Photonic crystal nanobeam cavity strongly coupled to the feeding waveguide

Qimin Quan, Parag B. Deotare, and Marko Loncar

Citation: Applied Physics Letters **96**, 203102 (2010); doi: 10.1063/1.3429125
View online: http://dx.doi.org/10.1063/1.3429125
View Table of Contents: http://scitation.aip.org/content/aip/journal/apl/96/20?ver=pdfcov
Published by the AIP Publishing

Photonic crystal nanobeam cavity strongly coupled to the feeding waveguide

Qimin Quan,[a)] Parag B. Deotare, and Marko Loncar
School of Engineering and Applied Sciences, Harvard University, Cambridge, Massachusetts 02138, USA

(Received 4 February 2010; accepted 15 March 2010; published online 17 May 2010)

A *deterministic* design of an ultrahigh Q-factor, wavelength-scale photonic crystal nanobeam cavity is proposed and experimentally demonstrated. Using this approach, cavities with $Q > 10^6$ and on-resonance transmission $T > 90\%$ are designed. The devices, fabricated in silicon and capped with a low refractive index polymer, have experimental $Q = 80\,000$ and $T = 73\%$. This is, to the best of our knowledge, the highest transmission measured in deterministically designed, wavelength-scale high-Q cavities. © *2010 American Institute of Physics*. [doi:10.1063/1.3429125]

Photonic crystal (PhC) (Refs. 1 and 2) cavities, with quality (Q) factors over 1×10^6 and wavelength-scale mode volumes, are widely applied in fields that range from quantum information processing and nonlinear optics to biomedical sensing. Theories based on Fourier space analysis,[3,4] multipole cancellation,[5] and mode-matching mechanisms[6–8] have been developed to explain the origin of the high Q factors. The design of PhC cavities, however, is typically based on an extensive parameter search and optimization,[9–13] also known as intuitive design. The large computational cost, in particular the computation time, needed to perform the simulation of high-Q cavities makes this trial-based method inefficient. Inverse design engineering, in which the physical structure is optimized by constructing specific target functions and constraints, has also been proposed.[14,15] A design recipe based on the desired field distribution is proposed in Ref. 16. In this paper, we propose and experimentally demonstrate a *deterministic* method to design an ultrahigh Q, wavelength-scale PhC nanobeam cavity (Fig. 1) that is strongly coupled to the feeding waveguide (i.e., near unity resonance transmission). The design approach is deterministic in the sense that it does not involve any trial-based hole shifting, resizing and overall cavity rescaling to ensure the ultrahigh Q-factor of the cavity. Moreover, the final cavity resonance has less than a 2% deviation from the targeted frequency. Our design method requires only computationally inexpensive, photonic band calculations (e.g., the plane wave expansion method), and is simple to implement.

The Q factor of a PhC nanobeam cavity can be maximized by reducing the out-of-plane scattering (Q_{sc}) due to coupling to radiation modes. As shown previously,[3,16] the scattered power (P_{sc}) can be expressed as an integral of the spatial Fourier frequencies within the light cone, calculated over the surface above the cavity: $P_{sc} \propto \int_{<\text{lightcone}} dk(|\text{FT}(H_z)|^2 + |\text{FT}(E_z)|^2)$, where FT denotes the spatial Fourier transform and z is the direction perpendicular to the surface. The integral is minimized when the major spatial Fourier components are tightly localized at the edge of the first Brillouin zone.[4] We start by considering the ideal field distribution on this surface which would minimize P_{sc}. We consider a nanobeam cavity consisting of a waveguide region of length L that supports propagating modes, bounded on each side by an infinitely long Bragg mirror [Fig. 1(a)]. Without loss of generality, we consider a TE-like cavity mode, which has H_z as a major field component. In the case of a conventional periodic Bragg mirror, the evanescent field inside the mirror can be expressed as $\sin(\beta_{\text{Bragg}} x)\exp(-\kappa x)$, where κ is the attenuation constant. The cavity field inside the waveguide region can be represented as $\sin(\beta_{\text{wg}} x)$. As mentioned above, the scattering loss decreases in the mirror section when $\beta_{\text{Bragg}} = \pi / a$, while phase matching between the mirror and waveguide,[7] $\beta_{\text{Bragg}} = \beta_{\text{wg}}$, minimizes the scattering loss at the cavity-mirror interface. The spatial Fourier transform of such a cavity field is approximately a Lorentzian function in the vicinity of π / a [Fig. 1(c)]. As proposed in Ref. 9, the energy of spatial harmonics within the light cone can be minimized (i.e., the Q factor maximized) if the field attenuation inside the mirror has a Gaussian shape $\sin(\beta_{\text{Gauss}} x)\exp(-\sigma x^2)$ [Fig. 1(d)]. Figure 1(e) shows the fraction of energy, η, associated with spatial harmonics within the light cone. Evidently, η for the cavity with a Gaussian attenuation is roughly two orders of magnitude smaller than that of the cavity with an exponential attenuation, and is minimized at $L = 0$. Therefore, the optimal cavity length for this type of cavity is zero, which simultaneously minimizes the mode volume (V) of the cavity, and thus increases Q/V. It is worth noting that $L/a = 3$ in Fig. 1(e) corresponds to the well-known L3 cavity.[9]

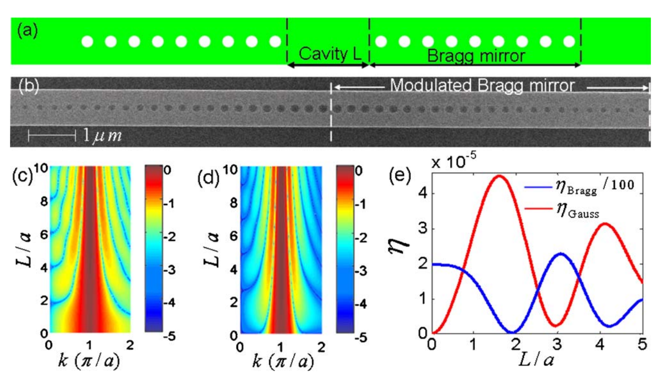

FIG. 1. (Color online) (a) Schematic of a nanobeam PhC with a conventional Bragg mirror. (b) SEM image of a silicon nanobeam PhC with a "modulated Bragg mirror." (c) $\log_{10}|\text{FT}(H_z)|$ for a model cavity with exponential attenuation ($\kappa = 0.6$) in the mirrors. (d) $\log_{10}|\text{FT}(H_z)|$ for a model cavity with Gaussian attenuation ($\sigma = 0.1$) in the mirrors. (e) The fraction of the Fourier components that are within the light line, assuming a refractive index ratio of 2.5 between the waveguide and the surroundings.

[a)]Electronic mail: quan@fas.harvard.edu.

The preferred Gaussian attenuation can be obtained from a Bragg mirror by making the mirror strength κ a linearly increasing function of the position within the mirror, i.e., $\kappa=\sigma x$. We name such a mirror a "modulated Bragg mirror." In the case of a dielectric-mode nanobeam cavity, this can be achieved by lowering the band edges of each mirror segment by linearly decreasing the filling fraction (FF). The FF is defined as the ratio between the hole area and the area of the unit cell. Note that other types of modulation may exist which enable a linearly increasing mirror strength. To prevent scattering, the oscillating part of the field, $\sin(\beta_{\mathrm{mod}}x)$, should have a constant β_{mod} throughout the mirror. This condition is satisfied only if each segment of the modulated Bragg mirror has the same length (periodicity) a, and if the operating frequency (cavity resonance) is kept inside the band gap of each segment. In such a structure, the resonant frequency of the cavity mode is very close to, but slightly lower than, the dielectric band edge of the central mirror segment. This can be attributed to the linearly decreasing FF of the mirror, which results in an increased overlap between the cavity mode and dielectric material. The frequency offset, which can be estimated using perturbation theory, decreases as the number of modulated mirror segments increases.

The design principles we have elaborated thus far can be summarized as follows: (i) the cavity length should be zero ($L=0$), (ii) the length of each segment should be the same (period$=a$), resulting in a constant phase velocity at π/a, and (iii) a modulated Bragg mirror results in an optimal Gaussian-shaped field attenuation. We demonstrate the power of this recipe by designing an ultrahigh Q-factor, small mode volume PhC nanobeam cavity that operates at 1525 nm (196.6 THz), that is strongly coupled to the feeding waveguide [Fig. 2(a)]. We design the nanobeam for fabrication on a silicon-on-insulator (SOI) wafer with a 220 nm thick Si device layer (constrained by our SOI wafer properties). The nanobeam is made of silicon (refractive index $n=3.46$), while the top and bottom cladding, as well as the holes, are made of material with $n=1.45$ (e.g., polymer, SiO_2). The low index cap is added as a protective layer for future applications. Our design approach is as follows: (i) We choose the period a by selecting n_{eff} (phase index of the Bloch mode) to be between $n_{\mathrm{Si}}=3.46$ and $n_{\mathrm{clad}}=1.45$. $n_{\mathrm{eff}}=2.5$ is a good compromise, resulting in $a=\lambda_0/2n_{\mathrm{eff}}\sim 300$ nm. We note, however, that any n_{eff} (and thus any periodicity) which opens a band gap can be used as a starting point to realize a high-Q cavity, assuming that a sufficiently slow modulation is used. (ii) Next, we choose the width of the nanobeam to be as wide as possible, in order to push the mode away from the light line. Meanwhile, the second order Bloch mode (of the same symmetry as the fundamental mode) should be prevented from entering into the band gap. A band diagram simulation[17] shows that a width of 700 nm is an optimal choice. (iii) We find the FF which yields a dielectric band edge at 1.525 μm. With $n_{\mathrm{eff}}=2.5$, the FF can be estimated using the relation $1/n_{\mathrm{eff}}^2=(1-\mathrm{FF})/3.46^2+\mathrm{FF}/1.45^2$,[18] which gives 0.19. A band diagram simulation shows the actual FF=0.15 [Fig. 2(b)]. Mirror strengths, for different FFs, can be calculated using $\sqrt{(\omega_2-\omega_1)^2/(\omega_2+\omega_1)^2-(\omega_{\mathrm{res}}-\omega_0)^2/\omega_0^2}$, where $\omega_2,\omega_1,\omega_0$ are the air band edge, dielectric band edge, and midgap frequency of each segment, respectively, and ω_{res} is the cavity

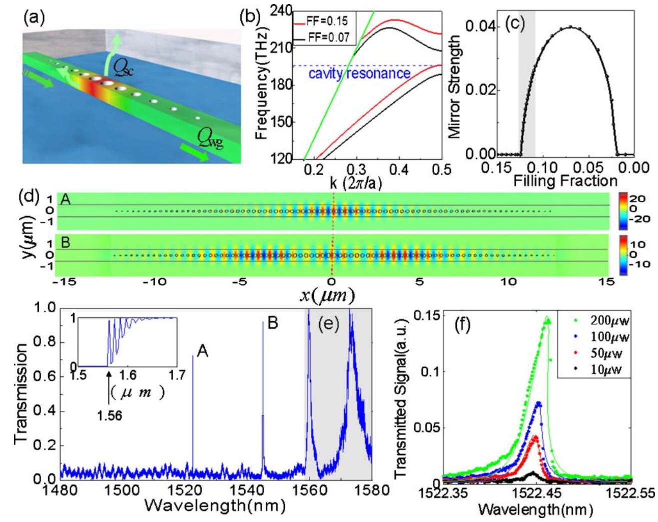

FIG. 2. (Color online) (a) Schematic of a modulated nanobeam cavity. Q_{wg} and Q_{sc} refer to energy loss due to the coupling to the feeding waveguide and scattering/radiation losses, respectively. (b) TE band diagrams for FF $=0.15$ and 0.07. The green line denotes the light line. The resonance of cavity mod40 is about 1.5% lower than the dielectric band edge of the central section with FF=0.15, due to the modulation. (c) Mirror strength for different FFs. An approximately linear increase is observed in the shaded region. (d) Simulated E_y profile at the middle of the nanobeam cavity for fundamental mode A ($Q_{\mathrm{A}}=2.7\mathrm{E}6$) and second mode B ($Q_{\mathrm{B}}=8\mathrm{E}4$). (e) Experimental transmission spectrum of the mod40 cavity with input power 100 μW. The signal is normalized by the band edge modes (shaded region), which have unity transmission, as verified by 3D-FDTD simulations shown in the inset. Due to the very large photon life time of our ultrahigh Q cavity ($\tau_{\mathrm{photon}}=Q/\omega\sim 1$ ns), it becomes nearly impossible to model transmission through the cavity (resonant tunneling) using the 3D-FDTD method directly. Hence, the high-Q cavity mode does not appear in the simulated spectrum shown in the inset. (f) Zoom-in of the transmitted signal of the fundamental mode at different input power levels (measured at the fiber tip). The dots are experimental data and the lines are the fitted curves using Eq. (1).

resonance. Linearly increasing mirror strength, needed for Gaussian type confinement, can be found in the shaded region in Fig. 2(c). (iv) Finally, the nanobeam cavity needs to be strongly coupled to the feeding waveguide in order to achieve a large transmission efficiency when probing the cavity. The transmission at the cavity resonance can be written as $T=Q_{\mathrm{total}}^2/Q_{\mathrm{wg}}^2$.[23] Therefore, in order to have $T\rightarrow 1$, total cavity Q-factor $[Q_{\mathrm{total}}=Q_{\mathrm{wg}}Q_{\mathrm{sc}}/(Q_{\mathrm{wg}}+Q_{\mathrm{sc}})]$ should be limited by Q_{wg}. The linear decrease in the FF from 0.15 to 0 provides a natural way to achieve this.

In the proposed design method (i)–(iv), all cavity parameters are determined using fast a few minutes long band diagram calculations only, and no trial-based parameter-search steps are needed. This significantly reduces the computational cost of the design process by several orders of magnitude. We emphasize that the most critical part of our design approach is to maintain a constant length of each mirror segment a, and to achieve a "tapered" mirror strength by decreasing the FF of each segment. This approach preserves the phase velocity of each segment and is essential for the realization of high-Q cavities. Our design strategy has an additional important advantage over other types of PhC nanobeam cavities:[9–12,19–22] it provides a natural way to strongly couple the cavity to the feeding waveguide.

To verify our designs, a 3D-FDTD simulation is used to study the cavity with the above-mentioned parameters. The results are summarized in Table I for two cavities with 40 and 50 modulated mirror segments on each side. It can be

TABLE I. 3D-FDTD simulation results of a waveguide-coupled cavity with 40 and 50 modulated mirror segments on each side of the cavity. The FF is changed from 0.15 at the center of the cavity to 0 at the edge. To calculate partial quality factors, we monitored the power flowing outside the cavity through closed surface enclosing the cavity. Q_{wg} was found by monitoring the power coupled into the waveguide and projecting it onto the fundamental mode of the waveguide. Q_{total} found using partial Qs was in good agreement with Q_{total} calculated directly by monitoring time decay of the cavity field. The transmission is obtained using Q_{total}^2/Q_{wg}^2. V_{eff} is the mode volume normalized by $(\lambda_0/n)^3$ where $n=3.46$ for silicon.

Type	λ (μm)	Q_{sc}	Q_{wg}	Q_{total}	V_{eff}	Trans.
mod40	1.552	2.20×10^7	1.25×10^6	1.19×10^6	1.1	0.91
mod50	1.549	2.46×10^7	2.18×10^7	1.16×10^7	1.2	0.29

seen that cavities feature ultrahigh Q-factors (both Q_{sc} and Q_{wg}), while at the same time giving a high transmission, particularly in cavity "mod40." In principle, the Q factors can be made arbitrarily high by applying a sufficiently slow modulation, at the cost of a larger mode volume. However, in practice the cavity Q-factor is limited by material losses and fabrication imperfections, and therefore, a design Q in the range of 10^7 is sufficient.

To experimentally verify our designs, we fabricated a waveguide-coupled cavity (mod40 design) in a SOI wafer with a 220 nm device layer on a 2 μm buried oxide using the fabrication procedure described in our previous work.[19] A spot size converter[24] consisting of a 2×2 μm^2 cross-section polymer pad ($n_{pad}=1.58$) was used to couple light in and out of the cavities using a tapered optical fiber. Since we are motivated by the biosensing applications of our cavities, we cover the cavities with a protective chemically-inert polymer. Unfortunately, PMMA ($n=1.45$), assumed in the design phase, was found to be unsuitable, and therefore, the devices were covered with another, more robust, polymer with a refractive index $n_{clad}=1.34$. We found that the smaller refractive index of the top cladding compared to the simulated one slightly affects the performance of our cavities: using 3D-FDTD modeling we found that the cavity resonance is shifted to a smaller wavelength ($\lambda_{model}=1517$ nm), the cavity Q_{total} is 2.72E6, and the on-resonance transmission is $T=75\%$.

We characterized the device by scanning a tunable laser source from 1470 to 1580 nm. A tapered fiber (2.5 μm spot diameter) is used to couple light in and out of the polymer waveguide. A polarizer is placed at the output to filter out the TM-like mode. Figure 2(e) shows the experimental transmission spectrum through one of the resonators. A nonlinear bistable lineshape is observed, as shown by the power-dependent spectra in Fig. 2(f). We fitted the experimental data using the following expression, typical of a nonlinear bistability:

$$T=\frac{P_{out}}{P_{in}}=\frac{Q_{total}^2/Q_{wg}^2}{1+[P_{out}/P_0-2(\lambda-\lambda_0)/\gamma_0]^2}, \quad (1)$$

where $P_0=3gQ_{total}Q_{wg}[\omega/(2nc)]^2\chi^{(3)}$ is the measured power in the presence of a third-order nonlinearity, g is a nonlinear feedback parameter introduced by Soljacic *et al.*,[25] and γ_0 is the natural cavity linewidth. $g\sim1/V_{eff}$ is a measure of the field confinement in the nonlinear region. From the fits, we obtained an experimental $Q=80\,000$ and an on-resonance transmission $T=73\%$ for the on-substrate and polymer-capped cavity. This corresponds to a $Q_{sc}=500\,000$, which is comparable to our previously reported results for a free-standing PhC nanobeam cavity.[19] The demonstrated transmission is much higher than previous work on a cavity with a similar Q factor.[26,27]

In summary, we have proposed and demonstrated a deterministic design of a high-Q PhC nanobeam cavity. Our cavity design is ideally suited for coupling to the feeding waveguide, and thus allows for a remarkably high transmission. As such, the cavity is an ideal candidate for the realization of densely integrated photonic systems, and is suitable for applications ranging from optical interconnects to biochemical sensors. Finally, the record high Q/V ratios of PhC nanobeam cavities will enable further fundamental studies in spontaneous emission control, nonlinear optics, and quantum optics.

We greatly acknowledge helpful discussions with M.W. McCutcheon. We thank J. Gong and N. Yu for the help in preparation of the front cover image. This work is supported by NSF under Grant No. ECCS-0701417 and NSF CAREER grant. Device fabrication is performed at the Center for Nanoscale Systems (CNS) at Harvard.

[1] E. Yablonovitch, Phys. Rev. Lett. **58**, 2059 (1987).
[2] S. John, Phys. Rev. Lett. **58**, 2486 (1987).
[3] J. Vuckovic, M. Loncar, H. Mabuchi, and A. Scherer, IEEE J. Quantum Electron. **38**, 850 (2002).
[4] K. Srinivasan and O. Painter, Opt. Express **10**, 670 (2002).
[5] S. G. Johnson, S. Fan, A. Mekis, and J. D. Joannopoulos, Appl. Phys. Lett. **78**, 3388 (2001).
[6] M. R. Watts, S. G. Johnson, H. A. Haus, and J. D. Joannopoulos, Opt. Lett. **27**, 1785 (2002).
[7] M. Palamaru and P. Lalanne, Appl. Phys. Lett. **78**, 1466 (2001).
[8] P. Lalanne, S. Mias, and J. Hugonin, Opt. Express **12**, 458 (2004).
[9] Y. Akahane, T. Asano, B. S. Song, and S. Noda, Nature (London) **425**, 944 (2003).
[10] B. S. Song, S. Noda, T. Asano, and Y. Akahane, Nat. Mater. **4**, 207 (2005).
[11] S. Tomljenovic-Hanic, C. M. de Sterke, and M. J. Steel, Opt. Express **14**, 12451 (2006).
[12] E. Kuramochi, M. Notomi, S. Mitsugi, A. Shinya, T. Tanabe, and T. Watanabe, Appl. Phys. Lett. **88**, 041112 (2006).
[13] M. Notomi, E. Kuramochi, and H. Taniyama, Opt. Express **16**, 11095 (2008).
[14] J. M. Geremia, J. Williams, and H. Mabuchi, Phys. Rev. E **66**, 066606 (2002).
[15] M. Burger, S. J. Osher, and E. Yablonovitch IEICE Trans. Electron. **E87-C**, 258 (2004).
[16] D. Englund, I. Fushman, and J. Vuckovic, Opt. Express **13**, 5961 (2005).
[17] All simulations are performed with Lumerical FDTD Solutions.
[18] K. Sakoda, *Optical Properties of Photonic Crystals*, 2nd ed. (Springer, Berlin, 2005).
[19] P. B. Deotare, M. W. McCutcheon, I. W. Frank, M. Khan, and M. Lončar, Appl. Phys. Lett. **94**, 121106 (2009).
[20] M. W. McCutcheon and M. Loncar, Opt. Express **16**, 19136 (2008).
[21] Y. Zhang and M. Loncar, Opt. Express **16**, 17400 (2008).
[22] J. Chan, M. Eichenfield, R. Camacho, and O. Painter, Opt. Express **17**, 3802 (2009).
[23] J. D. Joannopoulos, S. G. Johnson, J. N. Winn, and R. D. Meade, *Photonic Crystals: Molding the Flow of Light*, 2nd ed. (Princeton University Press, Princeton, 2008).
[24] S. J. McNab, N. Moll, and Y. A. Vlasov, Opt. Express **11**, 2927 (2003).
[25] M. Soljacic, M. Ibanescu, S. G. Johnson, Y. Fink, and J. D. Joannopoulos, Phys. Rev. E **66**, 055601(R) (2002).
[26] L. D. Haret, T. Tanabe, E. Kuramochi, and M. Notomi, Opt. Express **17**, 21108 (2009).
[27] Md. Zain, N. P. Johnson, M. Sorel, and R. M. De La Rue, Opt. Express **16**, 12084 (2008).